

# Influence of skin/core debonding on free vibration behavior of foam and honeycomb cored sandwich plates

Vyacheslav N. Burlayenko<sup>a</sup>, Tomasz Sadowski<sup>b,\*</sup>

<sup>a</sup>Department of Applied Mathematics, Engineering and Physical Faculty, National Technical University 'KhPI', 21 Frunze St., 61002 Kharkov, Ukraine

<sup>b</sup>Department of Solid Mechanics, Faculty of Civil and Sanitary Engineering, Lublin University of Technology, 40 Nadbystrzycka St., 20-128 Lublin, Poland

## ARTICLE INFO

### Article history:

Received 31 October 2008

Accepted 7 July 2009

### Keywords:

Debonding

Sandwich plates

Free vibration analysis

Finite element predictions

## ABSTRACT

The dynamic behavior of partially delaminated at the skin/core interface sandwich plates with flexible cores is studied. The commercial finite element code ABAQUS is used to calculate natural frequencies and mode shapes of the sandwich plates containing a debonding zone. The influence of the debonding size, debonding location and types of debonding on the modal parameters of damaged sandwich plates with various boundary conditions is investigated. The results of dynamic analysis illustrated that they can be useful for analyzing practical problems related to the non-destructive damage detection of partially debonded sandwich plates.

© 2009 Elsevier Ltd. All rights reserved.

## 1. Introduction

The use of sandwich composite structures has many potential applications in a variety of engineering fields. The sandwich structures correspond to the material system that includes three components such as the sandwich core, the face sheets or skins and film adhesive layer (Fig. 1).

This structural design concept offers additional advantages over the use of conventional engineering materials. Compared to monolithic composite laminates or metals, the sandwich concept significantly reduces weight and increases stiffness while maintaining strength. Even higher strength and stiffness properties can be achieved by increasing the thickness of the core  $h_c$  without a weight penalty. This excellent strength-to-weight ratio of sandwich materials with both honeycomb and foam cores can be used in a variety of engineering considerations for higher speed, longer range and greater payload capacity or reduced power demand, all of which are extensively exploited in aerospace and maritime applications, etc. [1]. Nevertheless, the current applications of them remain mainly limited to secondary components. Such “exploitation with caution” is caused by a proneness of the sandwich structures to a wide range of defects and damage [2] because of natural complex build-up and high influence of manufacturing processes on sandwich material quality. To manufacture sandwich panels, the face sheets should be

bonded by the film adhesive layer to the core. It is usually made by the co-cure process in the autoclave under appropriate vacuum bag pressure [3]. The manufacturing defects like incomplete wetting or entrapped air pockets into resin-dominant layer can result in non-uniform adhesion between the face sheets and the core or a skin-to-core debonding. Moreover, the local separation of the principal sandwich layers in isolated area can appear as a consequence of accidental tool drops during maintenance operations or can be attributable to in-service circumstances such as low velocity impact by foreign objects [4,5]. Besides, the partial interface degradation of the sandwich structure can be caused by water absorption ability of cellular cores [6] and outgassing from foam cores under direct sunshine exposition [7]. Overloading and elevated temperature regime can induce debonding at the weakest point of the skin-to-core interface, too.

The damage state associated with the existence of debonding has been found to affect a structural integrity of sandwich structures, reduces their overall stiffness and strength and modifies their dynamic responses [11–21] because the sandwich concept is locally lost (Fig. 2). Moreover, under in-service loading regimes debonding can propagate and trigger new damage modes such as face sheet wrinkling, face sheet delamination, core shear cracks, etc. (Fig. 2). These damage modes may interact between themselves and lead to a premature failure of structures under load levels lower than the designed threshold.

Because many structures using sandwich materials require extremely high level of reliability, debonding must be detected immediately after its occurrence to ensure the safety and durability of the structures. The presence of debonding can be identified by the

\* Corresponding author. Tel.: +48 81 5384386; fax: +48 81 5384173.

E-mail address: [t.sadowski@pollub.pl](mailto:t.sadowski@pollub.pl) (T. Sadowski).

certain non-destructive damage detection methods [8]. The vibration-based damage detection techniques are potentially a very attractive methodology of non-destructive tests (NDT) among them [9]. These techniques take any construction as a dynamic system and analyze its dynamic responses such as natural frequencies, mode shapes, modal damping, etc. Since debonding directly affects structural responses, their variations may be interpreted as a signal of damage occurrence as well as can be used to locate and to define severity extent of defects in the structural system. Therefore, the vibration-based damage monitoring provides a promising method for identifying debonding within sandwich structures. Although experimental investigations are often utilized for detection procedure, damage simulation using an accurate and efficient modeling technique can be helpful in reducing the number of expensive tests, e.g. [10]. Numerous studies for the free vibration of delaminated composite plates have been reported in the literature, however, only few investigations of debonding effects on vibration characteristics of sandwich plates have been conducted.

This paper focuses on the analysis of debonding in relation to its: size, location and form influence on the modal parameters of damaged sandwich plates with different internal composition (honeycomb core and PVC closed-cell foam one) and for various boundary conditions. The natural frequencies and mode shapes of the sandwich plates over the wide range of different types of debonding are computed to illustrate the usefulness of the present 3D finite element model for analyzing practical problems related to the vibration of damaged sandwich plates.

## 2. State of the art

A debonded area in an interfacial adhesive joint of sandwich panels or debonding is analogous to a delamination issue of laminate ones. Related studies on the free vibration of delaminated composite beam-plates are a field attracting the interest of many researchers. Ramkumar et al. [11] first studied this problem. Their model neglected the bending–extension coupling induced by delamination on the natural frequencies of delaminated structures. The improved

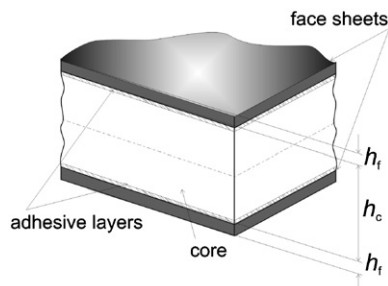


Fig. 1. Principal layers of a sandwich material.

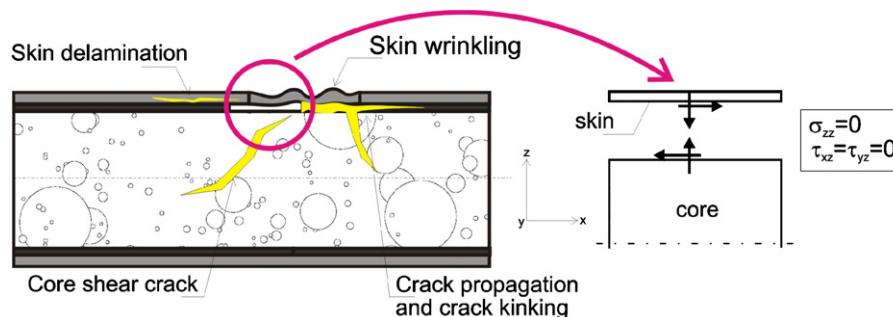


Fig. 2. Scheme of a section of a debonded sandwich plate.

‘free model’ of Wang et al. [12] gave a better agreement with experimental frequencies but it included physically unreal overlapping. The ‘constrained mode model’ in contrast to the ‘free model’ was proposed by Majumdar and Suryanarayn [13] and later adopted by Tracy and Pardoan [14]. However, this model excludes the possible opening vibration modes found by Shen and Grady [15]. Tenek et al. [16] presented a 3D finite element method to analyze the dynamic behavior of delaminated composite plates. They assumed that the gap between delaminated plies is infinitely small. Chen [17] studied the vibration of delaminated plates with two different types of models, a constrained model for vibrations in prebuckled states and a free model for vibration in postbuckled states. Ju et al. [18] carried out finite element analysis in conjunction with the Mindlin plate theory to analyze the effect of delamination on the free vibration of composite plates. It was found that the effect of delamination on natural frequencies is mode dependent and in some cases delamination may have significant effect on natural frequencies, even though the mode shapes of the plate are not significantly affected by delamination. The transverse shear effect is considered in his free model formulation. The effect of local thickening caused by delamination on vibration response was investigated by Hou and Jeronimidis [19]. They showed that this effect increases with the increase of delamination area of these plates and in many cases makes the frequencies of damaged plates even higher than that of the original undamaged plates. From their point of view the delaminated, unsupported areas of the plies are sufficiently flexible in bending to allow an increase in the local separation with associated geometrical stiffening of the plate as a whole, in spite of the decrease in the elastic properties of the damaged material. The comparison of experimental frequencies in CFRP sandwich panels damaged by debonding with numerical ones obtained by using NASTRAN code was presented by Paolozzi and Peroni [20]. The layerwise model for modeling composite laminate plates with embedded multiple delaminations was used by Kim et al. [21]. To model delamination, the delaminated element with the additional nodal unknowns was developed. Krueger [22] developed a 3D shell modeling technique for delaminations in composite laminates using the commercial software ABAQUS with 4-noded quadrilateral elements. Virtual/artificial spring elements was utilized by Yam et al. [23] to simulate the interface between upper and lower sublaminates in the delaminated region of laminated composite plates. Thereby, the investigation of internal or hidden damage in composite material is critical in engineering practice. This technique is especially important for monitoring of current state of damage of different parts of helicopters and aircrafts during the period of their exploitation.

## 3. Modeling

Numerical simulations by the finite element method have been used in most of the above mentioned publications due to difficulty to

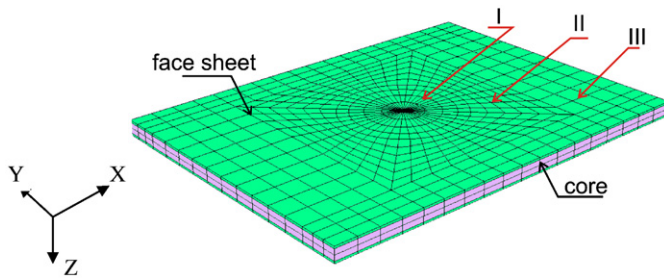


Fig. 3. Typical finite element mesh of a debonded plate.

obtain accurate analytical solution for this sandwich plate problem. The computational approach based on the finite element method plays very important role in the implement of damage detection technique for sandwich composites. On the other hand dynamic characteristics resulting from numerical analysis can also be used to guide the further experimental studies.

A number of assumptions were adopted in this investigation to treat the debonding damage of free oscillated sandwich plates:

- debonding is modeled as an artificial flaw embedded into interface between the skin and the core of the sandwich plates;
- the debonded surfaces are in contact vertically, the piecewise spring model is applied;
- debonding is assumed to be predetermined before the vibrations start and to be constant during oscillations;
- the complex debonding geometry is idealized by regular forms such as circle, rectangle or ellipse;
- the underlying cores are assumed to be intact in all cases and the honeycomb core is treated as an orthotropic continuous material, whereas the foam core is presented by an isotropic one.

The modeling of sandwich plates and analysis of free vibration responses was carried out using commercial software ABAQUS/Standard Version 6.6 [24]. A parametric input file was developed to enable representation of various debonding configurations. The finite element model generation with partially automatic meshing allows obtaining results of free vibration analysis over wide range of debonding size and form. The use of 3D computational elements to predict the dynamic responses of plate-like sandwich structures is inconvenient because of the number or aspect ratio of the elements necessary to obtain numerical solutions. Thus, an accurate plate-shell model or mixed shell/solid model for sandwich structures is desirable [22]. The finite elements such as 6- and 8-noded general-purpose reduced integrated continuum shell elements (SC6R, SC8R) based on the first order shear deformation theory, 6- and 8-noded with incompatible mode linear solid elements (C3D6I, C3D8I) were applied to discretize the skins and the core of sandwich plates, respectively. In doing so, the 6-noded elements were applied in a small inner zone at the vertex of the debonded region to align the surrounding elements. The general mesh of the sandwich plate model was subdivided into three different zones: (I) the refine meshed debonded zone, (II) the next zone surrounding debonding with gradually decreased mesh density, and (III) the coarse meshed fully bonded zone in order to minimize CPU time (Fig. 3).

In order to link the skin elements to the core elements in the fully bonded region of the sandwich plate multi-point constrains (MPC) were imposed in all nodes, these nodes are denoted as single nodes. The lack of adhesion between the elements in the debonded region was modeled by removing of those constrains and, as a consequence, the double nodes appear in this zone (Fig. 4). The debonded region

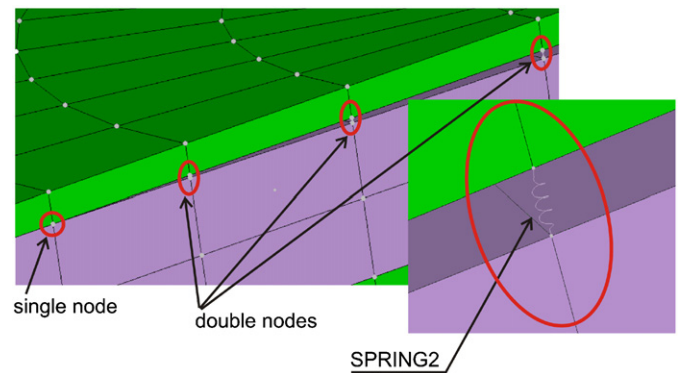


Fig. 4. Finite element mesh detail in the debonded zone.

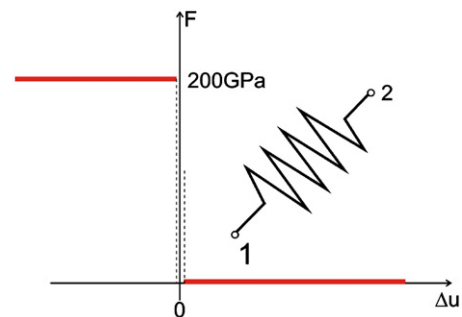


Fig. 5. Spring element constitutive law.

is modeled by creating a small gap (about 1% of face sheet thickness) between the face sheet and the core. To prevent the debonded face sheet from overlapping with the core and to model opening and closing of the interfacial damage in the vibration state, 3D spring elements SPRING2 were introduced between the double nodes in the debonded area (Fig. 4). The spring stiffness was taken as an arbitrary value between zero in the tension and very big stiffness in compression when relative transverse displacement  $\Delta u$  goes to zero (Fig. 5). Because the influence of the friction properties on the dynamic responses is negligible [25], the contact friction was assumed as equal to zero.

The macroscopic mechanical properties of a honeycomb sandwich panel depend on cell geometry, cell size ( $D$ ), cell wall thickness ( $t$ ) and height of the core ( $h$ ). With the purpose to simplify the modeling difficulties, related to naturally complex 3D finite element model of the cellular honeycomb structure, the sandwich core was replaced by homogeneous orthotropic material using the homogenization technique. The effective material properties of the honeycomb core were calculated using FE approach based on the unit cell conception [26,27]. For the regular hexagonal honeycomb core with unit cell dimensions, applied as  $D = 3$  mm,  $t = 0.025$  mm and  $h = 5$  mm and made up the foil material with Young's modulus  $E = 72$  GPa, density  $\rho = 2770$  kg m<sup>-3</sup> and Poisson's ratio  $\nu = 0.31$ , the properties of the homogenized honeycomb core are specified in Table 1.

Divinycell H grade polyvinyl chloride (PVC) closed-cell foams [28] used typically as core materials for marine sandwich structures were chosen by an alternative to the honeycomb core for the investigations. Divinycell H grade foams are supplied by the manufacture as plate-like panels in a wide range of thicknesses and densities. In the paper two types of foam core material referred as Divinycell H100 and H200 with densities 100 and 200 kg m<sup>-3</sup>, respectively, were used. The properties of the foam core materials are predominantly

**Table 1**  
Material properties of the sandwich plate components.

Material	Material constants
Aluminum honeycomb	$E_x = 0.461 \text{ MPa}$ , $E_y = 0.461 \text{ MPa}$ , $E_z = 1.494 \text{ GPa}$ , $G_{xy} = 0.194 \text{ MPa}$ , $G_{xz} = 341.7 \text{ MPa}$ , $G_{yz} = 192.1 \text{ MPa}$ , $\rho = 57.17 \text{ kg m}^{-3}$
PVC foam H 100	$E = 105.0 \text{ MPa}$ , $G = 45.0 \text{ MPa}$ , $\nu = 0.32$ , $\rho = 100 \text{ kg m}^{-3}$
PVC foam H 200	$E = 230.0 \text{ MPa}$ , $G = 85.0 \text{ MPa}$ , $\nu = 0.33$ , $\rho = 200 \text{ kg m}^{-3}$
CFRP	$E_x = 140 \text{ GPa}$ , $E_y = E_z = 10 \text{ GPa}$ , $G_{xy} = G_{xz} = 4.6 \text{ GPa}$ , $G_{yz} = 3.8 \text{ GPa}$ , $\nu = 0.25$ , $\rho = 1650 \text{ kg m}^{-3}$
Adhesive resin	$E = 1.5 \text{ GPa}$ , $G = 0.5 \text{ GPa}$ , $\nu = 0.40$ , $\rho = 141.31 \text{ kg m}^{-3}$

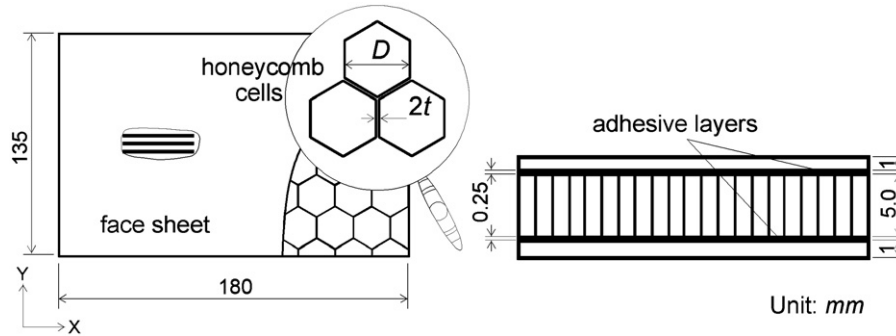


**Fig. 6.** Model of a honeycomb sandwich plate.

treated as homogeneous quasi-isotropic material [29] and are given in the Table 1.

#### 4. Numerical results

The numerical results of the FE analyses were obtained to provide insight and understanding of the free oscillation behavior of sandwich plates partially damaged at the skin/core interface. The free vibration analyses were performed using linear perturbation load step within ABAQUS software, where the Lanczos or the subspace iteration method for eigenvalues extraction were used [24]. Influences of debonding presence on the modal characteristics were assessed by comparisons of dynamic responses between a healthy sandwich plate and plates containing debonded zone. The FE predictions of the plates with different boundary conditions and core types as well as with various size or form of debonding are presented in details below.

##### 4.1. Convergence study

First, a convergence study was carried out to obtain values of natural frequencies as accurately as possible at the minimum number of elements required with the view to optimize computational time. A rectangular sandwich plate used for this purpose consisted of unidirectional CFRP face sheet material and aluminum honeycomb core. The fiber orientation angle of CFRP was zero degree to the longitudinal axis. The dimensions of the sandwich plate are pointed out in Fig. 6.

The material properties used for numerical simulation are shown in Table 1. For the free vibration analysis a perfect free boundary conditions were imposed around of all plate edges. The experimental data of the first torsional and bending modes of this sandwich plate were investigated in [30] and, thereby, were used to compare against the numerical calculations performed with ABAQUS. The FE mesh of the plate finally accepted due to convergence studies contained 2478 elements and 14908 nodes. Comparisons between numerical and experimental results for first torsional and bending eigenfrequencies are shown in Table 2, and the numerical results in contour plot form for the first six modes are presented in Fig. 7. Good agreements

**Table 2**  
Comparison between experimental and numerical results.

First torsional mode (Hz)			First bending mode (Hz)		
Analysis	Experiment [30]	Error (%)	Analysis	Experiment [30]	Error (%)
637.7	603.4	5.7	1300.1	1212.8	7.9

indicating a successful modeling of eigenvibration problem can be seen. Therefore, it validates the correctness of the FE model used within this investigation.

##### 4.2. Effect of debonding size

From the static analysis it is well-known that the size of a debonded region within sandwich panels influences the fraction of load transferred through the damaged region and, thereby, the debonding size strongly effects the final failure mode. The influence of the debonding size on the dynamical responses of sandwich plates has been presented as an indicator of sensitivity to the internal damage (discontinuities). To examine this effect on the sandwich plate, parametric studies over a wide range of debonding sizes were carried out. The FE model of the perfectly free rectangular honeycomb sandwich plate containing circular debonded region at the center was considered. The dimensions and material properties of the plate are taken the same as in the mentioned above convergence study. The planar size of prescribed debonding was defined by a damage parameter  $D\%$  denoting the ratio of the area of the debonded region  $A_d$  to the total area of the sandwich plate  $A_{total}$

$$D\% = \frac{A_d}{A_{total}} \cdot 100\% \quad (1)$$

Comparing natural frequencies of an intact plate and plates with pre-existing debonding, shifts in natural frequencies are usually observed. Results presented in Fig. 8 show the absolute value of the shifts in natural frequencies calculated for the case  $D\% = 15\%$  with increasing the mode numbers. It is obvious that shift on the higher modes is greater than the lower ones. Also, the shift in natural frequencies does not exhibit monotonous trends as mode number

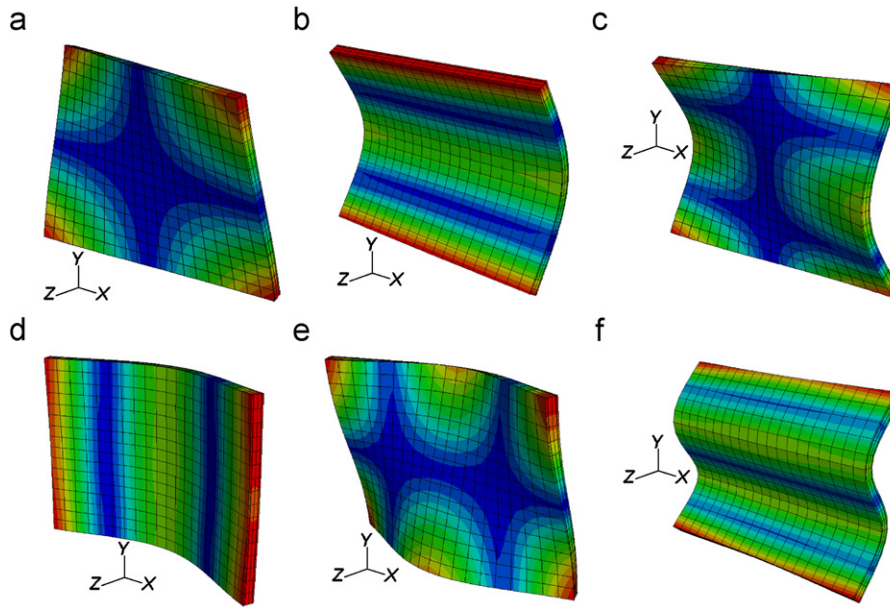


Fig. 7. Numerical eigenmodes of an intact sandwich plate: (a)  $\Omega = 637.7$  (Hz), (b)  $\Omega = 1300.1$  (Hz), (c)  $\Omega = 1803.0$  (Hz), (d)  $\Omega = 2449.6$  (Hz), (e)  $\Omega = 2675.6$  (Hz), (f)  $\Omega = 3244.4$  (Hz), (g)  $\Omega = 3244.4$  (Hz).

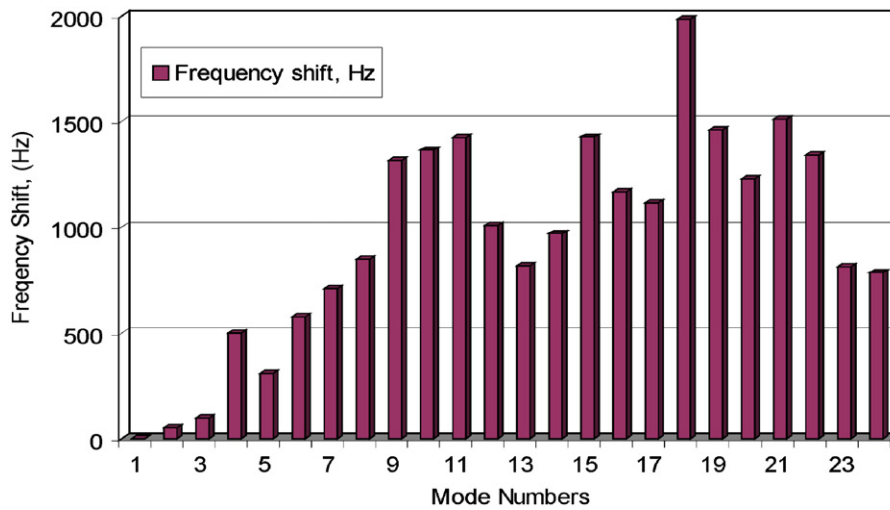


Fig. 8. Shift in natural frequencies.

increases. Moreover, as seen from Fig. 9, the mode shapes are definitely affected by the presence of debonding. The differences between the first six mode shapes of the healthy plate (Fig. 7) and the plate with central circular debonding (Fig. 9) are clearly observable in the contour plots. From Fig. 9 one can see that the modes of the damaged plate along with global deformed form contain the local deformation of the debonded region. This effect is more remarkable for higher natural frequencies.

The radius of the debonded region of the damaged plates was varied from 9 to 63 mm that corresponded to a variation of damage parameter from 1% to 50%. The diagram of the debonded region size expressed by the damage parameter vs. natural frequencies (the first eight) is shown in Fig. 10. It can be seen that the natural frequencies generally decrease with the increase of debonded area, while the first torsional mode is practically insensitive to the presence of debonding. Besides, from Fig. 10 one can also see that the presence of

relatively small area of debonding ( $D < 5\%$ ) does not almost change the lower natural frequencies, and decreases the higher natural frequencies only, although this tendency may be slightly violated due to effect of local thickening [19], for instance, eighth mode. However, the influence of debonding becomes more visible with the increasing of the radius of the circular debonded zone. In these cases even the first bending frequency is diminished up to 30%.

As it was mentioned above, the existence of the local oscillations of the debonded zone along with the global modes leads to changes of the mode shapes of these plates. In doing so, more remarkable this effect is for higher natural frequencies, but increasing of the debonded area leads to the appearance of such effect for lower frequencies. For instance, the inversion between the order of mode shapes, co-called cross-over phenomenon [20], was numerically obtained for the sixth and seventh modes when the damage parameter was more 10%, but it was observed for the third and fourth modes

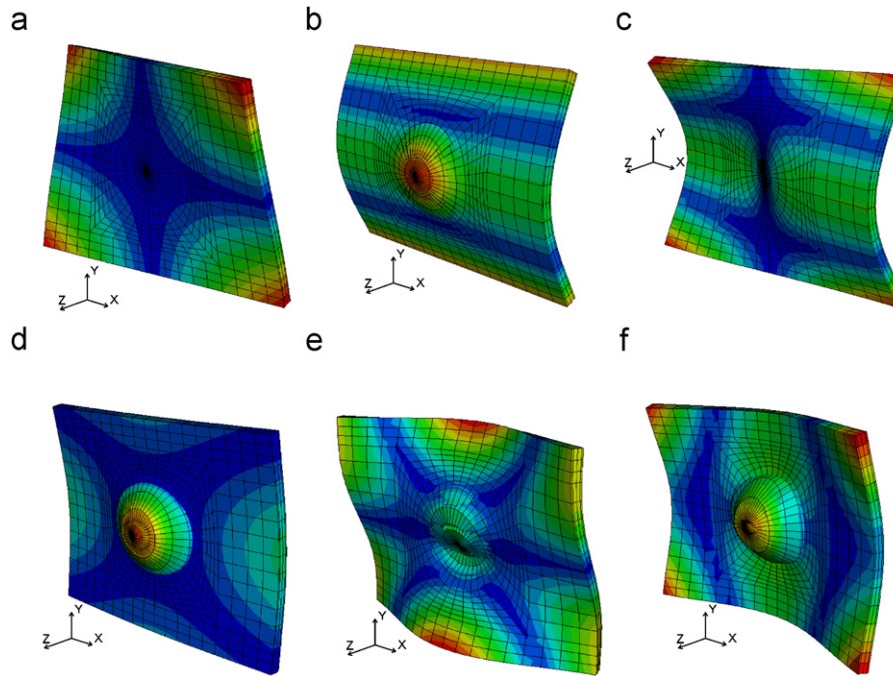


**Fig. 9.** Numerical eigenmodes of the plate with central debonding at the center: (a)  $\Omega = 636.1$  (Hz), (b)  $\Omega = 1263.3$  (Hz), (c)  $\Omega = 1707.3$  (Hz), (d)  $\Omega = 1961.9$  (Hz), (f)  $\Omega = 2379.8$  (Hz), (g)  $\Omega = 2685.7$  (Hz).

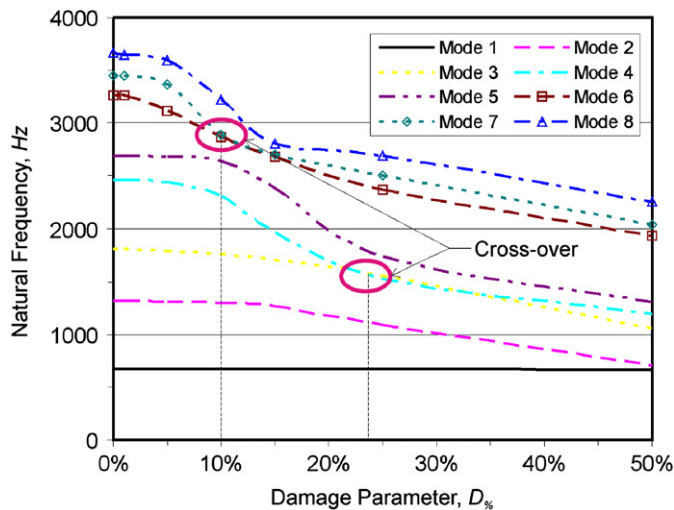


**Fig. 10.** Numerical eigenfrequencies as a function of debonded area.

after 20% of the damage value (Fig. 10). Thus, through observation of such sudden changes in the vibration modes, the location and severity of debonding may be identified.

#### 4.3. Effect of boundary conditions

It is well-known, that boundary conditions can help to highlight the importance of localized effects in structural responses of panels. The influence of boundary conditions on the free vibration of the sandwich plates damaged by debonding was studied by comparing the natural frequencies for four different types of the boundary conditions, namely such as FFFF, SSSS, CSCS and CCCC, where by 'F' is denoted the free edge of the plate, 'S' and 'C' represent the simply supported and clamped edges, respectively. The material properties

and plates geometry were not changed compared to the previous calculations. The numerical results that emphasize the effect of the boundary conditions on the first four natural eigenfrequencies of the rectangular honeycomb sandwich plates with circular debonded region at the center are summarized in Fig. 11. Comparing the absolute value of the shifts in natural frequencies varying due to increasing of the damage parameter one can conclude that the increase of the shift in fundamental frequency follows the increase of the debonding size and it significantly increases with the greater constraining of the plate. Thus, the greatest shift in fundamental frequency is reached for the fully clamped plate. This trend remains the same for all four eigenfrequencies. Though, the difference between the variations of the third frequency for the cases of CSCS and CCCC is insignificant. Moreover, the fundamental frequency as well as other three frequencies of the debonded plate shift from the healthy one more or less unaffected due to the constraining when the debonding parameter is a very small ( $D < 5\%$ ). But for its moderate and especially large size, the frequencies shift considerably if the constraining goes towards enhancement. Thereby, the presence of debonding within the sandwich plates can be detected by imposing of the corresponding boundary conditions more easily, when the debonding size is not very small.

#### 4.4. Effect of core types

To study the effect of a core type on the free vibration responses, three simply supported square plates of approximately the same weight but consisting of different core materials such as heavy H200 and light H100 PVC foams and stiffer honeycomb structure were investigated. The material properties are listed in Table 1 and their geometrical data are given in Table 3. The finite element predictions for the first four modes associated with the corresponding core material are compared in Fig. 12. It can be seen from Fig. 12 that the shift of the natural frequencies has trend to be similar in pattern for both light and heavy foam cores but differs from honeycomb one at the same debonding size. This is due to the change in the system

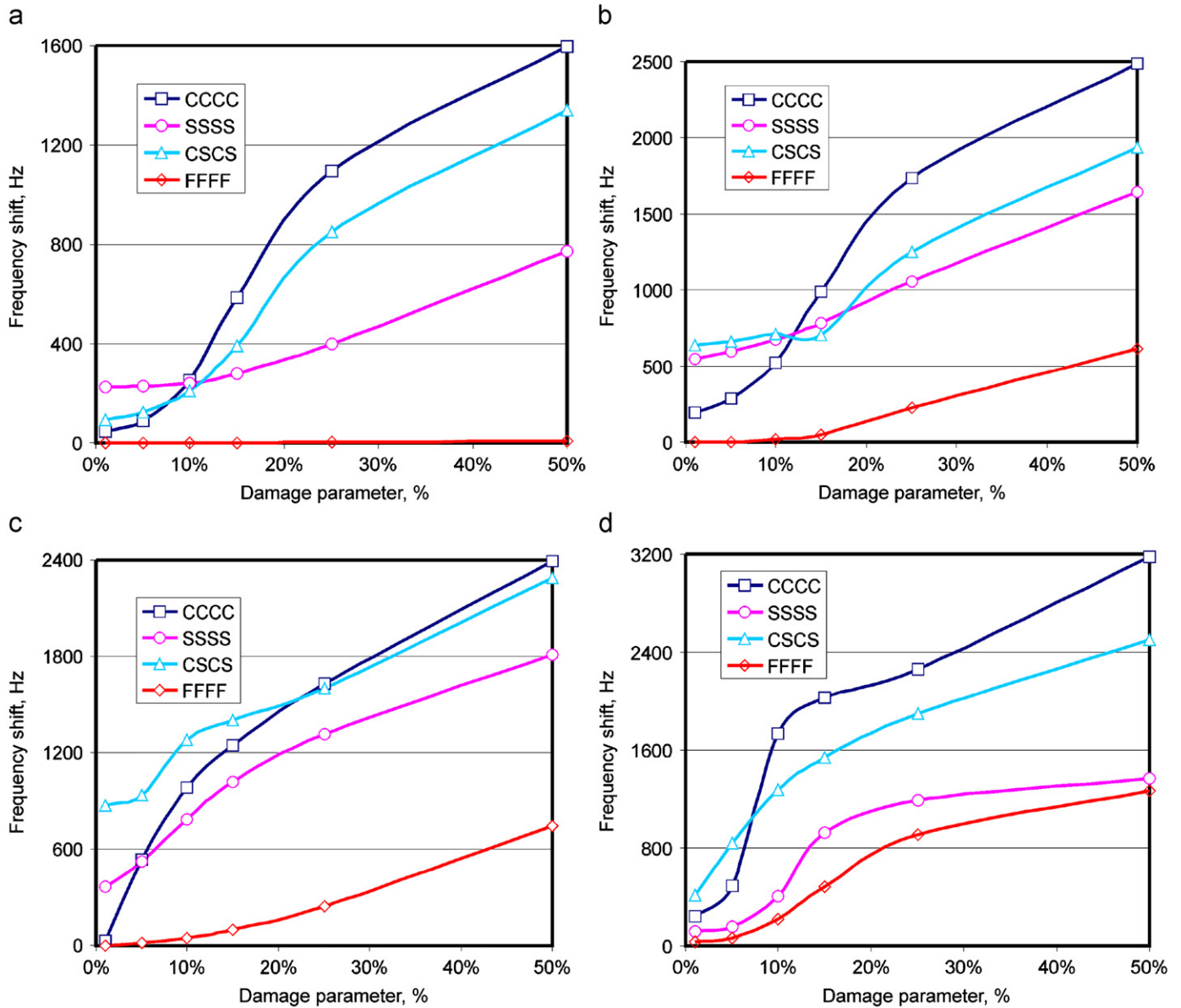


Fig. 11. Numerical eigenfrequencies vs. damage parameter for various boundary conditions: (a) first mode, (b) second mode, (c) third mode, and (d) fourth mode.

**Table 3**  
Geometrical properties of the sandwich plates components.

	CFRP/CORE/CFRP		
	CFRP/H100	CFRP/H200	CFRP/honeycomb
$h_f$ (mm)	1.235	1.0	1.325
$h_c$ (mm)	15.1	16.0	14.7

stiffness caused by the change in the properties of the core materials. As can be seen from this figure, the frequency shifts increase with increase of the core stiffness, particularly for the first and third modes such effect is more observable. Consequently, the stiffer system was investigated, the higher its sensitivity was observed to the existence of internal damage, for instance, debonding defects. It is also noted that the natural frequencies of the debonded plate shift from the healthy one independently from the core material, more when the

debonding area is relatively large. Besides, this effect of debonding on natural frequencies is mode dependent and varies with vibration modes. Such observations can be useful in the development of damage indices for debonding detection using vibration techniques.

4.5. Effect of debonding shape

In the final part, free vibration analyses of sandwich plates are studied to distinguish the effect of various debonding geometry. In order to model the different sensitivity of dynamic characteristics of the damaged sandwich plates to the debonding geometry, four types of finite element models have been developed (Fig. 13). The models corresponded to cases of damage extended as a circle, rectangle, ellipse and through the width of the plate, respectively.

Comparative analysis of several modes of the damaged sandwich plates are demonstrated in Fig. 4 where damage parameter  $D_0$  was varied as 1%, 5%, 15% and 25%, respectively. Simply supported

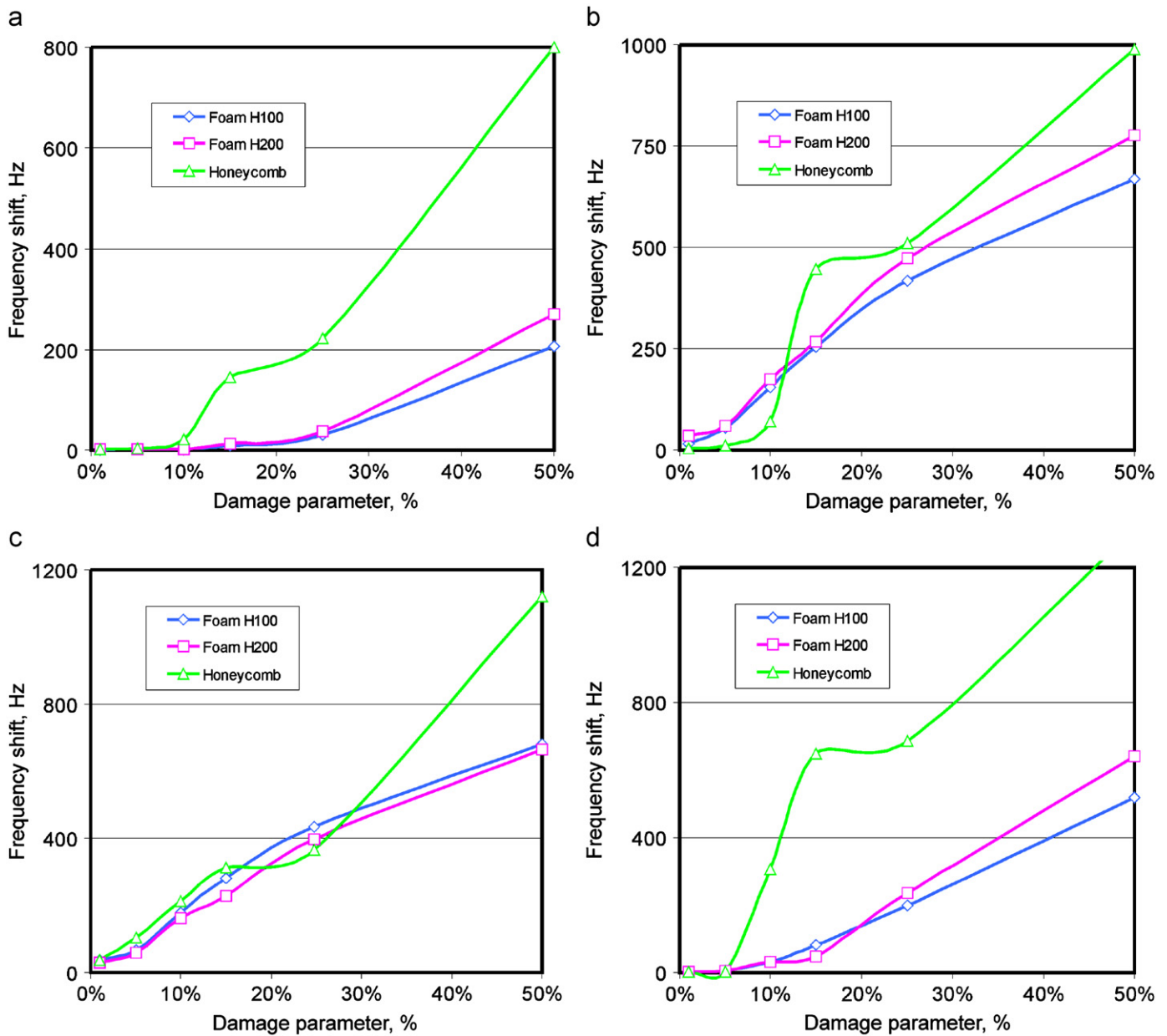


Fig. 12. Numerical eigenfrequencies vs. damage parameter for various core types: (a) first mode, (b) second mode, (c) third mode, and (d) fourth mode.

rectangular honeycomb sandwich plates with planar dimensions and thicknesses pointed out in Fig. 6 and consisting of CRFP face sheets and aluminum core (Table 1) were considered. Fig. 14 illustrates that the effect of debonding geometry, generally, has no regularity on the free vibration responses. As can be seen from this figure, the frequency shifts for all analyzed shapes of discontinuities increase with increase of the damage parameter. Nevertheless, in the average sense, the circular debonding geometry is more sensitive to the free oscillations of the sandwich plates.

**5. Conclusions**

The influence of the interfacial skin/core debonding on the vibration responses of damaged sandwich plates is studied by comparing numerical results of free vibration analyses both for intact and

debonded sandwich plates. Conclusive points from these investigations are the following:

- size of the debonding zone ( $D_{\%}$ ) strongly influences the sandwich plate response. The natural frequencies of debonded structure decrease due to loss in stiffness caused by existence of initial discontinuity. The mode shapes contain local deformations in the region of discontinuity. The influence of debonding becomes more visible with radius increase of the discontinuity zone. The cross-over phenomenon takes place in certain shape mode cases. The debonding size can be treated as an indicator of sandwich plate dynamic response sensitivity to the internal damage presence;
- boundary conditions imposed on investigated sandwich plate are very important. The analyzed rectangular plate examples can be treated as a fragment of bigger structural element of aircraft

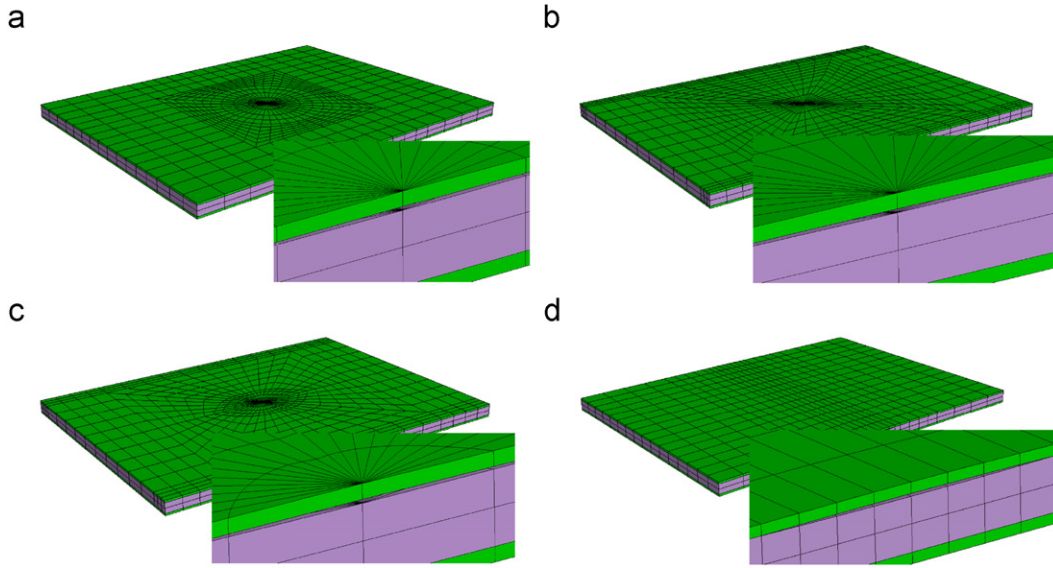


Fig. 13. Various forms of debonding geometry: (a) circular zone, (b) rectangular zone, (c) elliptic zone, and (d) through-the-width zone.

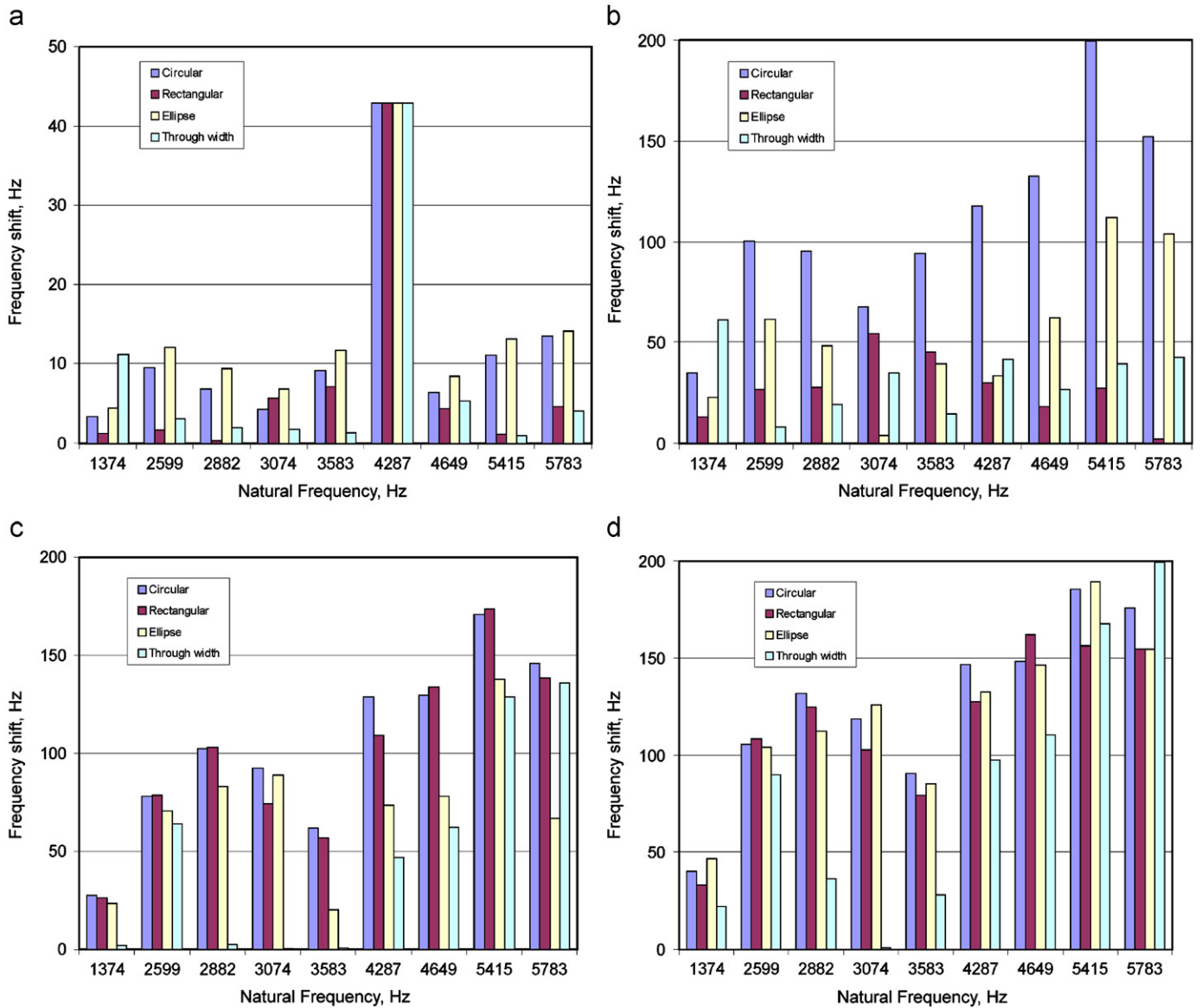


Fig. 14. Shift in natural frequencies for various debonding geometry cases: (a)  $D_x = 1\%$ , (b)  $D_x = 5\%$ , (c)  $D_x = 15\%$ , and (d)  $D_x = 25\%$ .

or helicopter. Joining of the analyzed plate with other parts of the structure can be modeled by different boundary conditions. Fig. 11 indicates that the maximum shift of fundamental frequency with radius increase of the debonding zone is in case of the fully clamped plate;

- core types of the sandwich plates strongly affect the dynamic structure response. Soft core made of light H100 PVC is less sensitive as for shift of the natural frequencies due to debonding presence. Application of heavy H200 PVC foam, what makes the whole sandwich structure stiffer, increases shift of the natural frequencies slightly in comparison to H100 PVC. However, the numerical results for honeycomb sandwich plate (much rigid in comparison to both previous cases) indicate that the response of stiff structure is significantly different, particularly for larger debonding defects;
- the shape of debonding region is other important parameter as for description of sandwich rectangular plate dynamic behavior. Different shapes of discontinuities influence in different way the different modes. In average sense one can state that the rectangular sandwich plates with the circular shape of debonding are more sensitive to free oscillations;
- higher natural frequencies and mode shapes are more sensitive to the debonding presence.

### Acknowledgments

This research is supported by Marie Curie Actions, ToK project-MTKD-CT-2004-014058 funded by European Union within the Sixth Framework Program. Financial support of Structural Funds in the Operational Programme - Innovative Economy (IE OP) financed from the European Regional Development Fund - Project No POIG.0101.02-00-015/08 is also gratefully acknowledged.

### References

- [1] J.R. Vinson, Sandwich structures, *Applied Mechanics Review* 54 (2001) 201–214.
- [2] J. Tomblin, T. Lacy, B. Smith, S. Hooper, A. Vizzini, S. Lee, Review of damage tolerance for composite sandwich aircraft structures, Technical Report DOT/FAA/AR-99/49, Office of Aviation Research, Washington, DC, 1999.
- [3] K.F. Karlsson, B.T. Aström, Manufacturing and application of structural sandwich components—part A, *Composites A* 28 (1997) 97–111.
- [4] D. Guedra-Degeorges, P. Thevenet, S. Maison, Damage tolerance of sandwich structures, in: *Proceedings of Euromech 360 Colloquium*, Kluwer Academic Publishers, Saint Etienne, 1977, pp. 29–36.
- [5] S. Abrate, Localized impact on sandwich structures with laminated facings, *Applied Mechanics Review* 50 (1997) 62–82.
- [6] J.E. Shafizadeh, J.C. Seferis, E.F. Chesmar, R. Geyer, Evaluation of the in-service performance behavior of honeycomb composite sandwich structures, *Journal of Materials Engineering and Performance* 8 (6) (1999) 661–668.
- [7] C. Berggreen, B.C. Simonsen, Non-uniform compressive strength of debonded sandwich panels—II: fracture mechanics investigation, *Journal of Sandwich Structures and Materials* 7 (2005) 483–517.
- [8] T.G. Gerardi, Health monitoring aircraft, *Journal of Intelligent Materials Systems and Structures* 1 (1990) 375–385.
- [9] O.S. Salawu, Detection of structural damage through changes in frequency: a review, *Engineering Structures* 19 (7) (1997) 18–23.
- [10] P. Cawley, R.D. Adams, A vibration technique for non-destructive testing of fiber composite structures, *Journal of Composite Materials* 13 (1979) 161–175.
- [11] R.L. Ramkumar, S.V. Kulkarni, R.B. Pipes, Free vibration frequencies of a delaminated beam, in: *34th Annual Technical Conference, Reinforced Plastic/Composite Institute, The Society of the Plastics Industry*, 1979, pp. 1–5.
- [12] J.T.S. Wang, Y.Y. Lin, J.A. Gibby, Vibration of split beams, *Journal of Sound and Vibration* 84 (1982) 491–520.
- [13] P.M. Majumdar, S. Suryanarayn, Flexural vibration of beams with delaminations, *Journal of Sound and Vibration* 125 (1988) 441–461.
- [14] J.J. Tracy, G.C. Pardoan, Effect of delamination on the natural frequencies of composite laminates, *Journal of Composite Materials* 23 (1989) 1200–1215.
- [15] M.-H.H. Chen, J.E. Grady, Free vibrations of delaminated beams, *AIAA Journal* 30 (1992) 1361–1370.
- [16] L.H. Tenek, E.G. Henneke II, M.D. Gunzburger, Vibration of delaminated composite plates and some applications to non-destructive testing, *Composite Structures* 23 (3) (1993) 253–262.
- [17] H.P. Chen, Free vibration of prebuckled and postbuckled plates with delamination, *Composites Science and Technology* 51 (3) (1994) 451–462.
- [18] F. Ju, H.P. Lee, K.H. Lee, Free vibration of composite plates with delamination around cutouts, *Composite Structures* 31 (1995) 177–183.
- [19] J.P. Hou, G. Jeronimidis, Vibration of delaminated thin composite plates, *Composite Part B* 30 (1999) 989–995.
- [20] A. Paolozzi, I. Peroni, Detection of debonding damage in a composite plate through natural frequency variations, *Journal of Reinforced Plastics and Composites* 9 (1990) 369–388.
- [21] H.S. Kim, A. Chattopadhyay, A. Ghoshal, Characterization of delamination effect on composite laminates using a new generalized layerwise approach, *Computers and Structures* 81 (2003) 1555–1566.
- [22] R. Krueger, A shell/3D modeling technique for delaminations in composite laminates, *Proceeding of American Society of Composites* (1999) 843–852.
- [23] L.H. Yam, Z. Wie, Z. Cheng, W.O. Wong, Numerical analysis of multi-layer composite plates with internal delamination, *Computers and Structures* 82 (2004) 627–637.
- [24] ABAQUS User Manual: Version 6.6, ABAQUS Inc. Pawtucket, Rhode Island, USA, 2006.
- [25] Y.W. Kwon, D.L. Lannamann, Dynamic numerical modeling and simulation of interfacial cracks in sandwich structures for damage detection, *Journal of Sandwich Structures and Materials* 4 (2002) 175–199.
- [26] M. Grediac, A finite element study of the transverse shear in honeycomb cores, *International Journal of Solids and Structures* 30 (3) (1993) 1777–1788.
- [27] V.N. Burlayenko, T. Sadowski, Analysis of structural performance of sandwich plates with foam-filled aluminum hexagonal honeycomb core, *Computational Materials Science* 45 (3) (2009) 658–662.
- [28] DIAB International AB: Eastville Close, Gloucester, Divinycell H: Technical Manual, 2007.
- [29] J.-M. Berthelot, E. Lolive, Non-linear behaviour of foam cores and sandwich materials—part 1: material and modeling, *Journal of Sandwich Structures and Materials* 4 (2002) 219–247.
- [30] Y. Tanimoto, T. Nishiwaki, T. Shiomi, Z. Maekawa, A numerical modeling for eigenfrequency analysis of honeycomb sandwich panels, *Composite Interfaces* 8 (6) (2001) 393–402.